JOURNAL OF CATALYSIS 147, 171–176 (1994)

CO Oxidation on Substituted Copper Chromite Spinel Oxide Catalysts

K. S. R. C. Murthy* and J. Ghose[1]

*Chemistry Department, Indian Institute of Technology, Kharagpur, Pin 721302, India; and *Microelectronics and Computer Division, Indian Telephone Industries, Ltd., Banglore, Pin 560016, India*

Received April 14, 1993; revised August 6, 1993

Oxidation of carbon monoxide was studied on Mg- and Al-substituted $CuCr_2O_4$ spinel catalyst at atmospheric pressure and temperatures between 373 and 723 K. The activity of $CuCr_2O_4$ decreased even for small replacements of either Cu by Mg or Cr by Al and none of the substituted oxides was as axtive as $CuCr_2O_4$.

In $Cu_{1-x}Mg_xCr_2O_4$ catalysts, the activity systematically decreased with increasing x, except for $0.4 < x < 0.6$. The decrease in activity is due to a decrease in the active Cu^{2+} ions of the catalyst. The increase in activity on increasing x from 0.4 to 0.6 is attributed to the crystallographic phase change, i.e., tetragonal to cubic, in the catalyst. This was also found in the $CuCr_{2-x}Al_xO_4$ catalysts. The decrease in the catalytic activity on substitution of Cr by Al, even when the total copper content is not altered, is due to the reduction of some of the active Cu^{2+} ions to Cu^{1+} ions.

INTRODUCTION

The normal spinel, $CuCr_2O_4$, is a very versatile catalyst, used in hydrogenation, dehydrogenation, dehydrocyclization, propellant combustion, decomposition of alcohols, nonaromatic hydrocarbon reforming, conversion of CO with H_2O or NO, as well as a number of oxidation reactions. Extensive studies on the mechanism of its catalytic activity have, however, not been undertaken, and the few reports published until now appear to be rather contradictory: the studies by Rastogi *et al.* (1) and Boldyreva *et al.* (2) have attributed the activity of the catalyst in the propellant combustion reaction to the presence of octahedral Cr^{3+} ions, whereas Hertl and Feranto (3) have reported that for CO oxidation the activity of Cr ions is only above 453 K, while that of Cu ions is below this temperature.

Thus, the present work was taken up in an attempt to understand the catalytic behaviour of copper chromite spinel oxide. In these studies, Cu^{2+} and Cr^{3+} of $CuCr_2O_4$ were progressively replaced by relatively inert Mg^{2+} (i.e., $Cu_{1-x}Mg_xCr_2O_4$) and Al^{3+} (i.e., $CuCr_{2-x}Al_xO_4$) ions, and the catalytic activities of these solid solutions in CO oxidation were determined.

[1] To whom correspondence should be addressed.

EXPERIMENTAL

The solid solutions $Cu_{1-x}Mg_xCr_2O_4$ (x = 0, 0.2, 0.4, 0.6, 0.8, and 1.0) and $CuCr_{2-x}Al_xO_4$ (x = 0, 0.2, 0.4, 0.6, 0.8, 1.0, 1.2, 1.4, 1.6, 1.8, and 2.0) were prepared by coprecipitating the metal ions as hydroxides with ammonia and subsequent calcination, as described earlier (4). The catalysts were characterised both before and after use by X-ray analysis. X-ray diffraction patterns of the samples were recorded with an X-ray unit model PW 1710 using Cu$K\alpha$ radiation (λ = 1.5418 Å) and a Ni filter. High-temperature X-ray diffraction patterns were taken using a Philips X-ray diffractometer (model No. MRC, X-96-N3), complete with high-temperature attachment. Differential thermal analysis (DTA) studies were carried out between 300 and 1273 K at a rate of 10 K/min using a VEB, DTA apparatus.

Surface areas of all the samples were determined using a Sorptometer (Carlo Erba, Model 1826) with nitrogen gas as adsorbate at liquid nitrogen temperature. The volume of nitrogen gas adsorbed at various equilibrium pressures and liquid nitrogen temperature was noted. Prior to each measurement, the sample was degassed under vacuum (5×10^{-3} Torr) at 473 K for 3 h. The surface area was calculated using the BET equation.

CO oxidation was carried out using a fixed-bed flow reactor at atmospheric pressure. The reactor was made of a pyrex glass tube 2.5 cm in diameter and 30 cm in length, fitted with a small inner glass tube concentric with the reactor tube for inserting the thermocouple.

In a typical run, about 1.5 g of catalyst powder was charged into the middle of the reactor between two plugs of pure pyrex glass wool. The reaction was carried out at temperatures between 373 and 723 K. The rates of gas flow used were air = 600 cm^3/min, CO = 30 cm^3/min. Before each run the reactor was heated to 673 K and flushed with purified argon gas (supplied by Indian Oxy-

0021-9517/94 $6.00

TABLE 1

Surface Areas of $Cu_{1-x}Mg_xCr_2O_4$ and $CuCr_{2-x}Al_xO_4$ Samples

Sample	BET surface area (m^2/g)	Sample	BET surface area (m^2/g)
$CuCr_2O_4$	20.3	$CuCr_{1.8}Al_{0.2}O_4$	17.6
$Cu_{0.8}Mg_{0.2}Cr_2O_4$	18.1	$CuCr_{1.6}Al_{0.4}O_4$	12.0
$Cu_{0.6}Mg_{0.4}Cr_2O_4$	20.7	$CuCr_{1.4}Al_{0.6}O_4$	13.6
$Cu_{0.4}Mg_{0.6}Cr_2O_4$	21.3	$CuCr_{1.2}Al_{0.8}O_4$	10.2
$Cu_{0.2}Mg_{0.8}Cr_2O_4$	25.6	$CuCrAlO_4$	11.0
$MgCr_2O_4$	28.2	$CuCr_{0.6}Al_{1.4}O_4$	16.1
		$CuCr_{0.4}Al_{1.6}O_4$	12.7
		$CuCr_{0.2}Al_{1.8}O_4$	13.2
		$CuAl_2O_4$	15.7

gen, Ltd.) at a rate of 2500 cm^3/min, and then the furnace was cooled to the experimental temperature. After the reactant mixture was fed into the reactor, the system was allowed to reach steady state (which took approximately 3–4 h) and then CO_2 was collected in the bubblers containing barium hydroxide. The amount of CO_2 in the effluent gas was calculated by estimating the unreacted barium hydroxide against standard hydrochloric acid using phenolphthalein indicator. The amount of CO in the feed and that of CO_2 formed after reaction were evaluated at STP conditions from which the percentage conversion per gram catalyst and conversion per cation were determined.

RESULTS

Specific surface areas of all the samples are given in Table 1. Fractions of the metal ions on the octahedral site of $CuCr_{2-x}Al_xO_4$ samples are shown in Table 2.

TABLE 2

Fractions of the Metal Ions on the Octahedral Site of $CuCr_{2-x}Al_xO_4$ Spinel Samples

Sample		Fractions of metal ions on B sites		
		Cu	Al	Cr
$CuCr_2O_4$	NA0	0	0	2
$CuCr_{1.8}Al_{0.2}O_4$	NA2	0.06	0.14	1.8
$CuCr_{1.6}Al_{0.4}O_4$	NA4	0.09	0.31	1.6
$CuCr_{1.4}Al_{0.6}O_4$	NA6	0.13	0.47	1.4
$CuCr_{1.2}Al_{0.8}O_4$	NA8	0.18	0.62	1.2
$CuCr_{1.0}Al_{1.0}O_4$	NA10	0.22	0.78	1.0
$CuCr_{0.6}Al_{1.4}O_4$	NA14	0.31	1.09	0.6
$CuCr_{0.4}Al_{1.6}O_4$	NA16	0.35	1.25	0.4
$CuCr_{0.2}Al_{1.8}O_4$	NA18	0.39	1.41	0.2
$CuAl_2O_4$	NA20	0.44	1.56	0.0

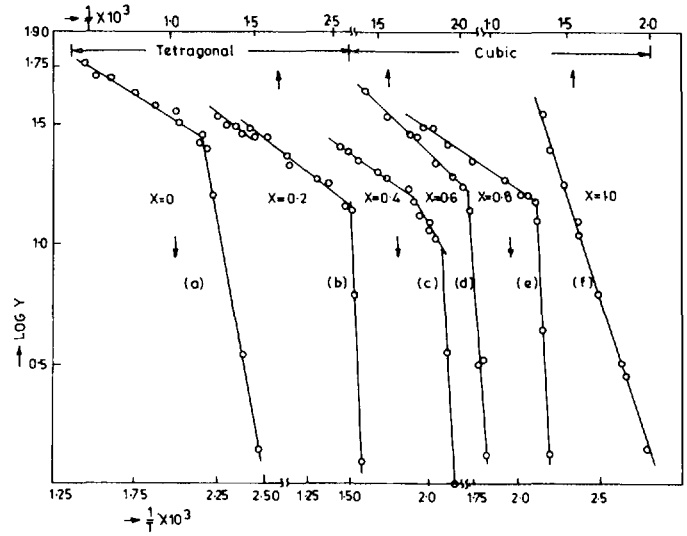

FIG. 1. Log Y vs $1/T$ plots (Y is the percentage of CO converted per g catalyst and T is the absolute temperature) for $Cu_{1-x}Mg_xCr_2O_4$ samples where x is (a) 0, (b) 0.2, (c) 0.4, (d) 0.6, (e) 0.8, and (f) 1.0.

The variation in percentage conversion (Y) of CO per 1 g catalyst with absolute temperature (T) between 373 and 723 K on various catalyst samples is indicated in Figs. 1 and 2. In these figures log Y is plotted against the reciprocal of absolute temperature ($1/T$). The plots for

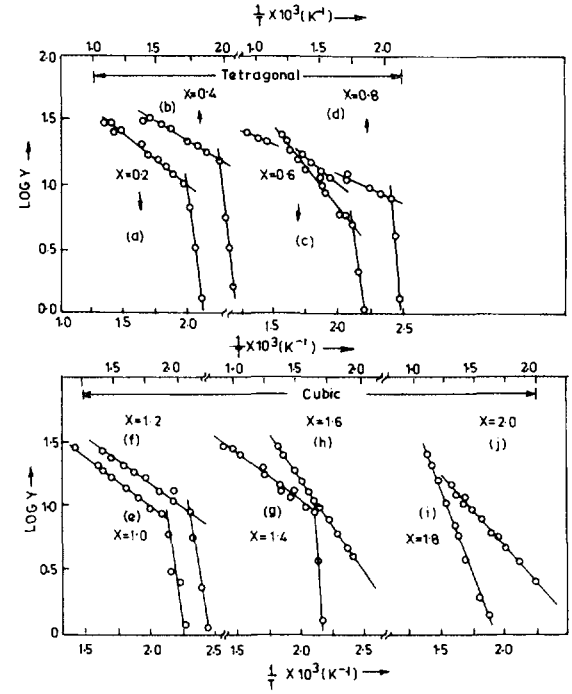

FIG. 2. Log Y vs $1/T$ plots for $CuCr_{2-x}Al_xO_4$ samples where x is (a) 0.2, (b) 0.4, (c) 0.6, (d) 0.8, (e) 1.0, (f) 1.2, (g) 1.4, (h) 1.6, (i) 1.8, and (j) 2.0.

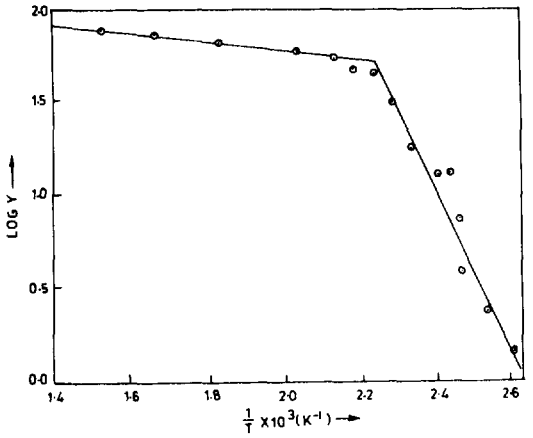

FIG. 3. Log Y vs $1/T$ plot for $CuCr_2O_4$ obtained by Hertl and Feranto (3).

$Cu_{1-x}Mg_xCr_2O_4$ samples, where x = 0, 0.2, 0.4, 0.6, 0.8, and 1.0, are shown in Figs. 1a–1f, while those for $CuCr_{2-x}Al_xO_4$ samples, where x = 0.2, 0.4, 0.6, 0.8, 1.0, 1.2, 1.4, 1.6, 1.8, and 2.0, are shown in Figs. 2a–2j.

The results show that the log Y vs $1/T$ plots of $Cu_{1-x}Mg_xCr_2O_4$ samples where x = 0.2, 0.4, 0.6, 0.8 (Figs. 1b–1e) and $CuCr_{2-x}Al_xO_4$ samples where x = 0.2, 0.4, 0.6, 0.8, 1.0, 1.2, 1.4 (Figs. 2a–2g) are similar in nature to the plot of pure $CuCr_2O_4$ (Fig. 3). The linear plots for these samples contain a break in the temperature range 453–498 K, below which the conversion increases rapidly with temperature. Above the break, the rate of this increase decreases. In Figs. 1b, 1c, 2c, and 2d an additional break in the log Y vs $1/T$ plots is observed above 500 K. Figures 1f, 2h, 2i, and 2j show that the log Y vs $1/T$ plots for these samples are linear without breaks. Conversions of the $Cu_{1-x}Mg_xCr_2O_4$ are between 3 and 63% in the studied temperature range, and the change with x is shown in Fig. 4. The plots of conversion per Cu ion are shown in Fig. 5. Figures 6 and 7 give the corresponding plots for $CuCr_{2-x}Al_xO_4$.

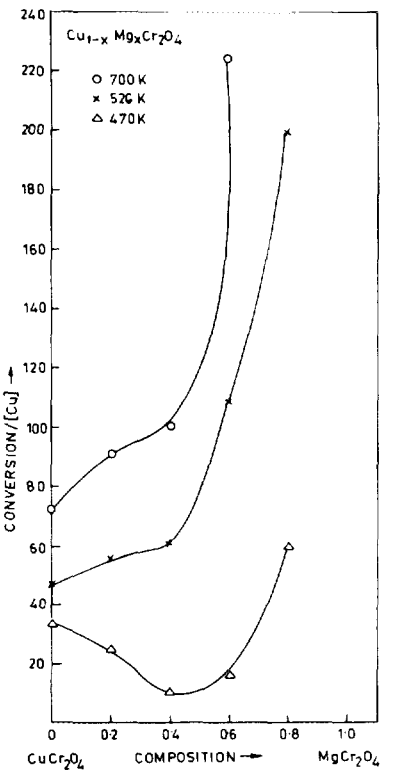

FIG. 5. Conversion per [Cu] ion as a function of catalyst composition for the system $Cu_{1-x}Mg_xCr_2O_4$ at different temperatures.

Figure 8 shows the change in the transition temperature with x in $CuCr_{2-x}Al_xO_4$ and $Cu_{1-x}Mg_xCr_2O_4$ solid solution samples from thermal analysis and high-temperature X-

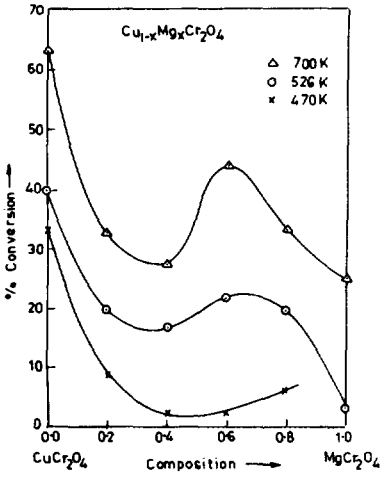

FIG. 4. Percentage conversion as a function of catalyst composition for the system $Cu_{1-x}Mg_xCr_2O_4$ at different temperatures.

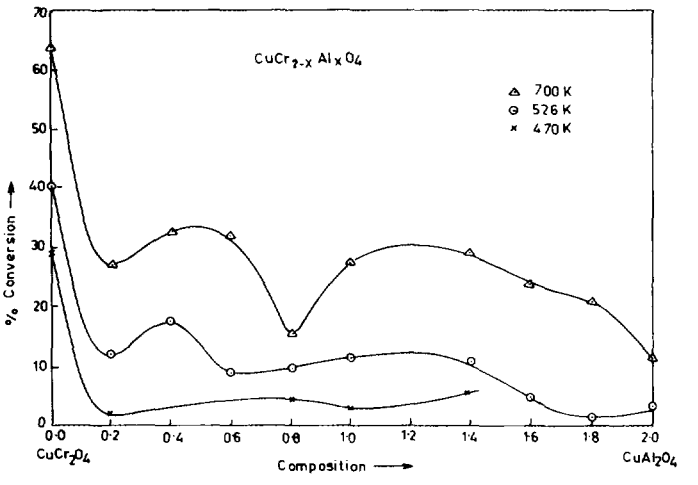

FIG. 6. Percentage conversion as a function of catalyst composition for the system $CuCr_{2-x}Al_xO_4$ at different temperatures.

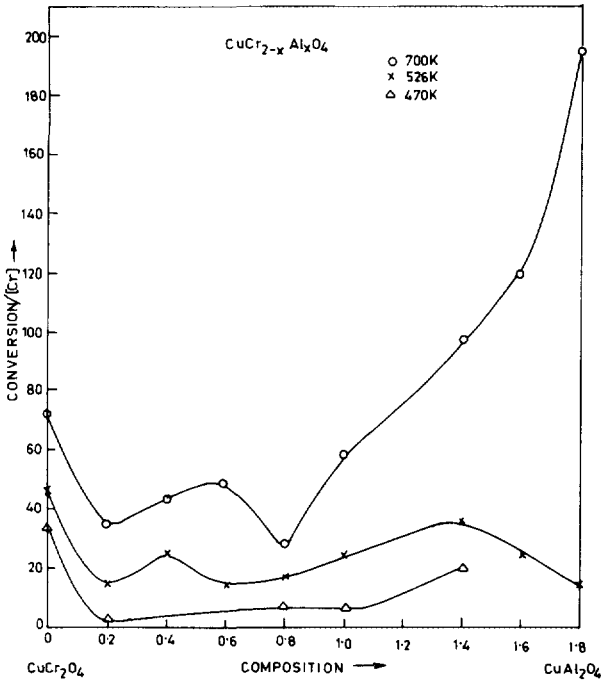

FIG. 7. Conversion per [Cr] ion as a function of catalyst composition for the system $CuCr_{2-x}Al_xO_4$ at different temperatures.

ray studies. Figure 9 shows the ESCA patterns of $CuCr_{1.8}Al_{0.2}O_4$ (NA2) and $CuCr_{1.2}Al_{0.8}O_4$ (NA8).

DISCUSSION

The results show that the log Y vs $1/T$ plot (Arrhenius plot, Fig. 1a) for the oxidation of CO on $CuCr_2O_4$ is similar to the plot obtained by Hertl and Feranto (3) (Fig. 3). From kinetic and IR studies, these authors have suggested that the catalytic action involving $CuCr_2O_4$ proceeds by two paths, one via the formation of unidentate carbonate groups, mainly on the surface Cr ions, and the other via the formation of metal carbonyl groups on the surface

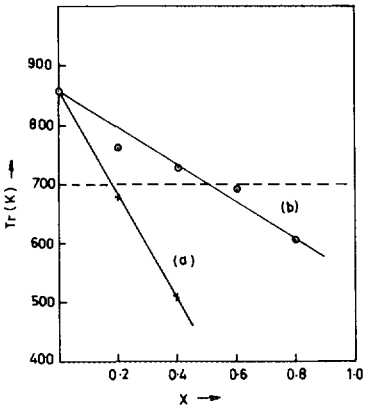

FIG. 8. Variation in tetragonal to cubic phase transition temperature with x for (a) $Cu_{1-x}Mg_xCr_2O_4$ (NM) and (b) $CuCr_{2-x}Al_xO_4$ (NA).

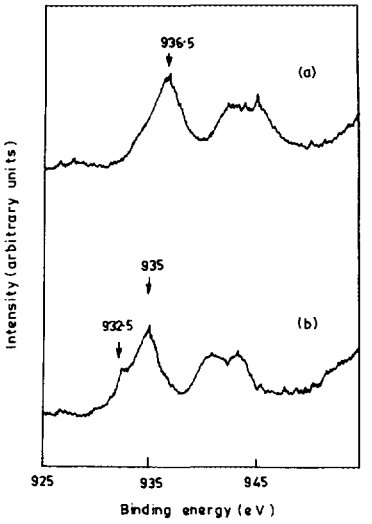

FIG. 9. Spectra for (a) $CuCr_{1.8}Al_{0.2}O_4$ (NA2) and (b) $CuCr_{1.2}Al_{0.8}O_4$ (NA8).

copper ions. They further reported that metal carbonyl groups react with gas-phase oxygen at temperatures between 353–453 K, while the unidentate carbonate groups react with oxygen at temperatures above 453 K to give CO_2, and the observed break in the Arrhenius plot at 453 K is due to this change in the reaction mechanism. Thus, any reduction in the copper content of the spinel catalyst should decrease its activity below 453 K, and above this temperature the activity should decrease with a reduction in the Cr content.

When Mg is substituted for Cu, the nature of the log Y vs $1/T$ plot does not change up to 80% replacement of Cu (Fig. 2), indicating that the oxidation mechanism remains unaltered when the copper content of the catalyst is reduced. However, when copper is completely replaced by Mg in the catalyst, i.e., $MgCr_2O_4$, the Arrhenius plot (Fig. 2f) shows a change, implying that the reaction mechanisms with $MgCr_2O_4$ as a catalyst and $CuCr_2O_4$ as a catalyst are not the same. The results in Fig. 4 show that the activity of $MgCr_2O_4$ is lower than that of $CuCr_2O_4$ at all temperatures between 373 and 673 K. However, Fig. 5 shows that the conversion per Cu ion increases, as more and more Cu is replaced by Mg except at lower temperatures, viz. 470 K. The increase in activity with decreasing copper content is expected for copper dilute catalysts, but when considerable quantities of Cu are present, this is quite unexpected and may indicate that at temperatures above ~500 K, the plots do not reflect the actual activity of the catalyst. Below 500 K, however, conversion and conversion per Cu ion (Figs. 4 and 5) both show a decrease up to $x = 0.4$ and then show an increasing trend. This is also the composition range, i.e., $0.6 < x < 0.4$ in which the spinel oxide samples change from cubic to tetragonal phase, as is evident from X-ray diffraction patterns. Thus,

at 470 K, the increase in activity on changing x from 0.6 to 0.4 may be associated with a crystallographic phase change in the catalyst. The effect of phase transition on the catalytic activity also seems to be evident in the log Y vs $1/T$ plots (Fig. 1), where the tetragonal samples show a break around the phase transition temperature recorded in the high-temperature X-ray studies (Fig. 8). This is also observed in the Al-substituted tetragonal samples, i.e., $CuCr_{2-x}Al_xO_4$ (Fig. 2). However, such a break is not observed in $CuCr_{2-x}Al_xO_4$ samples with $x = 0$, 0.2, and 0.4 (Figs. 1a, 2a, and 2b). This is expected, as the transition temperatures of these samples are above the studied temperature range, i.e., 723 K (Fig. 8).

A pronounced change in catalytic activity near the transition temperature of several solid substances undergoing crystallographic phase transition has been reported in the literature, although the influence of a bulk property like phase transition on the surface property like catalysis has not been unequivocally established. However, Krylov (5) has suggested that phase transition can exert some influence on the catalytic process, if the rate of phase transition is comparable to the rate of catalytic reaction.

DTA, X-ray diffraction studies, and electrical resistivity measurements on pure and substituted copper chromite samples have shown that the tetragonal to cubic phase transition in these spinel oxides are first order, diffusionless, reversible, and martensitic in nature, and proceed with high velocities (4). Kinetic studies on CO oxidation, with these spinel oxide catalysts have shown that CO_2 is produced at a very fast rate (1), implying that the reaction proceeds at very high speeds and may be comparable to the speed at which the tetragonal to cubic phase transition occurs in these catalyst samples, and hence a break is observed in the log Y vs $1/T$ plots. However, it cannot be fully ascertained that the break is due to phase transition, as *in situ* high-temperature X-ray patterns of the catalyst could not be taken. Also, the X-ray patterns of the used catalysts showed that the samples were not single-phase spinel oxides.

The plots of $CuCr_{2-x}Al_xO_4$ in Figs. 6 and 7 show that at all temperatures the plots of conversion and also conversion per Cr ion show decrease considerably when small amounts of Cr is replaced by Al. This is expected above ~500 K where the Cr ions of the catalyst are mainly taking part in the reaction, but below this temperature a decrease in the Cr content of the catalyst should not affect the conversion. However, such a decrease may occur if the active Cu ions change during the introduction of Al ions in the catalyst samples. Some recent studies on the mixed catalysts of Cu, Co, and Mn have shown that at the surface of the catalyst, Co and Cu ions are partially reduced by Mn ions, and this causes low activities of the Mn containing mixed oxides for CO oxidation (6). The lower activity of the Al-substituted $CuCr_2O_4$ catalysts may also be due to reduction of the active Cu^{2+} ions. Actually, such a possibility has been indicated in the thermoelectric power studies of $CuCr_{2-x}Al_xO_4$ samples. De *et al.* (4) have shown that in $CuCr_2O_4$ some of the Cr^{3+} ions are oxidised to Cr^{4+} ions, and the $CuCr_2O_4$ behaves as a p-type semiconductor where conduction is by hopping of charge carriers between Cr^{3+} and Cr^{4+} ions on the octahedral sites. Recently, Padmanaban *et al.* (7) have shown that the Al-substituted $CuCr_2O_4$ samples behave as compensated semiconductors in which Cu^{1+} ions, along with Cr^{4+} ions, are present. The presence of Cu^{1+} ions was detected in the ESCA studies. Figure 9 shows the Cu $2p3/2$ peaks for $CuCr_{2-x}Al_xO_4$ with $x = 0.2$ (NA2) and 0.8 (NA8). NA2 shows a peak at 936.5 eV which can be attributed to Cu_T^{2+} following D'Huyser *et al.* (8), who reported that Cu^{2+} on tetrahedral and octahedral sites of the spinel lattice show peaks at 936.2 ± 0.2 and 934.0 + 0.2 eV, respectively, and Cu^{1+} on tetrahedral and octahedral sites at 932.8 ± 0.2 and 931.3 ± 0.2 eV, respectively. The absence of a peak at 932.8 eV suggests that Cu^{1+} may not be present in NA2, but the results of thermoelectric power studies indicate the presence of Cu^{1+} ions in NA2 (7). The spectra of NA8, however, clearly show the presence of Cu^{1+} ions. This sample was chosen as it shows minimum catalytic activity for CO oxidation, and if Cu^{1+} ions are responsible for low activity, then NA8 is likely to have considerable amounts of Cu^{1+} ions and may be easily detected in the spectra. Figure 9 shows a peak at 932.5 eV corresponding to the reported peak for Cu_{tet}^{1+}. The spectra also show a peak at 935 eV which could be attributed to the presence of both Cu_{tet}^{2+} (~936.2 eV) and Cu_{oct}^{2+} (~934.0 eV). In NA2, a very small amount of Cu_{oct}^{2+} is present (Table 2); hence it shows a peak at 936.5 eV for Cu_{tet}^{2+} only. Thus in the $CuCr_{2-x}Al_xO_4$ catalysts, although the total copper content is not altered by substitution of Cr by Al, the amount of Cu^{2+} ions are reduced and hence there is a reduction in the catalytic activity. These results suggest that in the copper chromium spinel oxides the activity of Cu is due to Cu^{2+} ions.

Figure 7 shows that in the Cr dilute catalysts there is an increase in conversion per Cr ion as the Cr content is reduced, although conversion shows a decrease (Fig. 6). Such observations were also made by Egerton and Vickerman (9) on $MgCr_{2-x}Al_xO_4$. They attributed it to the varying degree of electron correlation between the surface Cr ions and its Cr nearest neighbours. The stronger this interaction is the less active the surface ion is. Cimino and Schiavello (10) also found the trend of an increase in activity per Ni ion as dilution increases in the $Ni_xMg_{1-x}Al_2O_4$ catalysts.

From these results it may be concluded that the catalytic activity of $CuCr_2O_4$ for the oxidation of CO is due to Cr ions above 500 K and the activity per Cr ion increases with Cr dilution due to weaker interactions of the

surface Cr ions with its near neighbours. The activity below 500 K is due to Cu^{2+} ions and their reduction to Cu^{1+} ions leads to a decrease in the catalytic activity.

REFERENCES

1. Rastogi, R. P., Singh, G., Dubey, B. L., and Shukla, C. S., *J. Catal.* **65,** 25 (1980).
2. Boldyreva, A. V., Mitrofanova, R. P., Boldyrev, V. V., Balakirev, V. F., Chufarov, G. T., and Pavlyukhin, Yu. G., *Fiz. Goreniya Vzryva* **11,** 715 (1975). [in Russian]
3. Hertl, W., and Feranto, R. J., *J. Catal.* **29,** 352 (1973).
4. De, K. S., Ghose, J., and Murthy, K. S. R. C., *J. Solid State Chem.* **47,** 264 (1983).
5. Krylov, O. V., *Kinet. Catal. (Engl. Transl.)* **22,** 9 (1981).
6. Yang, B. L., Chan, S. F., Chang, W. S., and Chem, Y. Z., *J. Catal.* **130,** 52 (1991).
7. Padmanaban, N., Avasthi, B. N., and Ghose, J., *J. Solid State Chem.* **81,** 250 (1989).
8. D'Huyser, A., Lerebours-Hannoyer, B. M., Lenglet, M., and Bonnelle, J. P., *J. Solid State Chem.* **39,** 246 (1981).
9. Egerton, T. A., and Vickerman, J. C., *J. Catal.* **19,** 74 (1980).
10. Cimino, A., and Schiavello, M., *J. Catal.* **20,** 202 (1971).